Research Square

Preprints are preliminary reports that have not undergone peer review.
They should not be considered conclusive, used to inform clinical practice,
or referenced by the media as validated information.

Nanosepiolite/MXene synergistically enhances the flame retardancy and mechanism of ethylene vinyl acetate copolymer with ammonium polyphosphate

Xuezheng Huang
20221001@huuc.edu.cn
Henan University of Urban Construction
Zhipeng Hou
Henan University of Urban Construction
Feng Liang
Henan University of Urban Construction
Junfeng Tian
Henan University of Urban Construction
Jianxi Li
CGN DELTA (Jiangsu) Plastic & Chemical Co., Ltd
Li Wu
Henan University of Urban Construction

Research Article

Keywords: Ethylene vinyl acetate copolymer, Ammonium polyphosphate, Nano sepiolite, MXene, Collaborative flame retardant

Posted Date: August 20th, 2026

DOI: https://doi.org/10.21203/rs.3.rs-10253544/v1

License: This work is licensed under a Creative Commons Attribution 4.0 International License.
Read Full License

Additional Declarations: No competing interests reported.

Nanosepiolite/MXene synergistically enhances the flame retardancy and mechanism of ethylene vinyl acetate copolymer with ammonium polyphosphate

Xuezheng Huang[1*] ,Zhipeng Hou[1] ,Feng Liang[1], Junfeng Tian[1],Jianxi Li[2],Li Wu[1]

1 Municipal and Environmental Engineering College, Henan University of Urban Construction, Pingdingshan, 467004, China

2 CGN DELTA (Jiangsu) Plastic & Chemical Co., Ltd., Suzhou 215400, PR China

*Correspondence:20221001@huuc.edu.cn

Abstract: In response to the problems of high addition of ammonium polyphosphate (APP) flame retardant ethylene vinyl acetate copolymer (EVA), easy cracking of carbon layer, and deterioration of mechanical properties, this study innovatively constructed an APP/nano sepiolite (NS)/MXene ternary synergistic flame retardant system. The multi-scale synergistic mechanism of the three components was revealed through systematic characterization using limiting oxygen index (LOI), cone calorimetry (CONE), thermogravimetric analysis (TGA), and scanning electron microscopy (SEM).The results showed that the LOI of the EVA-ASM sample with 20 wt% flame retardant (APP: NS: MXene=9.5:0.4:0.1) increased from 18% of EVA to 24.5%, the peak heat release rate (pHRR) decreased from 718 kW/m^2 of EVA to 308 kW/m^2, and the total heat release (THR) decreased from 91.7 MJ/m^2 to 74.7 MJ/m^2. NS fiber network and MXene layer respectively play the roles of "skeleton reinforcement" and "catalytic graphitization", synergistically forming a dense continuous carbon layer (residual carbon rate of 9.0%) with APP, effectively suppressing mass and heat transfer; The ternary system significantly improves the flame retardant performance while increasing the tensile strength from 4.0 MPa to 6.8 MPa, and maintaining a volume resistivity of over 10^{10} Ω· cm. This study provides a new strategy for developing high-performance flame-retardant EVA, which has potential applications in the field of new energy cable protection.

Keywords: Ethylene vinyl acetate copolymer; Ammonium polyphosphate; Nano sepiolite; MXene; Collaborative flame retardant

0 Introduction

Ethylene-vinyl acetate copolymer (EVA) is widely used in cable sheathing, photovoltaic encapsulation, footwear materials, and electronic equipment protection due to its lightweight nature, flexibility, and excellent processing properties [1-3]. However, EVA exhibits a limited oxygen index (LOI) of only 17-19%, classifying it as a highly flammable material. Its combustion process releases substantial heat and toxic smoke, posing serious threats to personnel safety and equipment reliability [4-5]. With the rapid development of the new energy industry, fields such as high-voltage cables, energy storage systems, and electric vehicles impose higher demands on the flame retardancy of EVA materials. Although traditional flame retardant technologies can enhance fire resistance, they often lead to deterioration in mechanical properties or increased environmental risks [6-8]. Therefore, developing efficient, environmentally friendly EVA composites with stable mechanical properties and enhanced flame retardancy has become a critical research topic in the field of polymer materials.

The intumescent flame retardant (IFR) system is considered an environmentally friendly solution due to its low smoke and low toxicity characteristics. Ammonium polyphosphate (APP), as the core component of IFR, acts through the synergistic effects of an acid source (decomposing to generate phosphoric acid), a gas source (releasing inert gases), and a carbon source (promoting char formation) [9]. This synergy facilitates the formation of an intumescent char layer on the material surface, effectively blocking heat and oxygen transfer [10]. However, the single APP/EVA system exhibits significant drawbacks: high loading levels (typically 25-35 wt%) severely compromise material flexibility; the char layer formed during combustion is prone to cracking, limiting flame retardant efficiency [11,12]; furthermore, the poor interfacial compatibility between APP and the EVA matrix can trigger filler agglomeration, further impairing the comprehensive performance of the material.

In recent years, the introduction of nanofillers (such as clay, layered double hydroxides, and two-dimensional materials) has provided new strategies to address these issues [13-15]. These materials can optimize the flame retardant pathway through mechanisms like physical barrier effects, catalytic char formation, or free radical trapping, while simultaneously enhancing the matrix's mechanical and thermal stability.

Among these, nano-sepiolite (NS) is a natural fibrous silicate mineral.It has excellent thermal stability and mechanical properties [16-18]. Its unique acicular structure, high specific surface area (200-300 m^2/g), and abundant surface silanol groups (Si-OH) confer excellent adsorption capacity and catalytic activity for char formation [19]. Studies show that NS can construct a three-dimensional network structure within the polymer matrix, delaying the diffusion of pyrolytic gases [20]. Moreover, it exhibits a synergistic effect with phosphorus-based flame retardants (e.g., APP), promoting the formation of a denser and more stable char layer. For instance, Liu et al [21]. reported that adding only 3 wt% NS to an APP/polypropylene system increased the LOI to 32% and significantly reduced the peak heat release rate (pHRR) by 40%. However, the flame-retardant enhancing effect of NS is constrained by its dispersion within the matrix and the interfacial bonding strength with the polymer; excessive addition tends to cause a decline in mechanical properties.

Meanwhile, MXene (e.g., $Ti_3C_2T_x$), an emerging two-dimensional transition metal carbide/nitride, demonstrates significant potential in polymer flame retardancy due to its high specific surface area, tunable surface functional groups (-OH, -O, -F), and intrinsic flame retardant properties [22]. The layered structure of MXene can effectively inhibit mass and heat transfer during combustion; its surface polar groups not only enhance interfacial interactions with the polymer but may also promote the graphitization of the char layer through catalytic oxidation, improving its barrier performance [23,24]. Existing research has confirmed a synergistic flame retardant effect between MXene and IFR systems [25]. However, the multi-scale synergistic flame-retardant mechanisms (such as physical barrier reinforcement, catalytic char enhancement, free radical quenching, etc.) between MXene and nano-sepiolite (NS) within an EVA matrix, particularly their synergistic enhancement on the flame retardant efficiency of APP, remain unclear. Therefore, systematically exploring the optimization pathways for flame retardancy, thermal stability, and mechanical properties of EVA using an APP/NS/MXene ternary composite system holds significant scientific merit and application value.

Based on this, the present study employs APP-flame-retarded EVA as the matrix

and constructs a highly synergistic ternary flame-retardant system (APP/NS/MXene/EVA) through the stepwise incorporation of nano-sepiolite (NS) and MXene. It aims to systematically investigate the influence of this system on the material properties. The specific research content includes: (1) Preparing APP/EVA reference samples and analyzing their fundamental flame retardant properties and char layer structural characteristics; (2) Introducing NS to prepare samples (APP/NS/EVA) and investigating the effect of NS content on regulating char layer compactness, heat release behavior, and mechanical properties; (3) Introducing MXene to prepare samples (APP/NS/MXene/EVA), focusing on elucidating the synergistic enhancement mechanism of MXene on the flame retardancy of the APP/NS/EVA system and its underlying micro-mechanisms. Characterization techniques including limiting oxygen index (LOI), cone calorimetry (CONE), thermogravimetric analysis (TGA), and scanning electron microscopy (SEM) will be employed to systematically analyze the pyrolysis behavior, char layer morphology evolution, and flame retardant mechanisms of the composites, establishing quantitative relationships between "composition-structure-properties".

1 Experiment

1.1 Main raw materials

Ethylene vinyl acetate copolymer (EVA), 40 L, DuPont, USA; Mxene，Multilayer, average particle size 5 um, Nangong Fenghui Nanotechnology Co., Ltd; Ammonium polyphosphate (APP), 1000 degree of polymerization, Guangzhou Runzhan Chemical Co., Ltd; Sepiolite, with an average particle size of 500 nm, produced by Hebei Runri Mineral Products Co., Ltd.

1.2 Main equipment and instruments

Double roll open mill, SK-160B，Dongguan Tin Testing Instrument Co., Ltd; Tablet machine, YST-100T，Dongguan Tin Testing Instrument Co., Ltd; Shore hardness tester, LX-D， Wenzhou Haibao Instrument Co., Ltd; High resistance meter, ZC-36，Shanghai Sixth Electric Meter Factory Co., Ltd; Microcomputer controlled electronic universal testing machine, ETM-A， Shenzhen Wance Testing Equipment Co., Ltd; X-ray diffractometer (XRD), D8 ADVANCE, Bruker AXS Corporation, Germany;

Scanning Electron Microscope (SEM), Phenom Pro, Phenom-world B.V., Netherlands; Differential scanning calorimeter, DSC822e, Mettler Toledo Switzerland; Thermogravimetric analyzer (TGA), Q50, TA Corporation, USA; Extreme Oxygen Index Tester, HC-2， Nanjing Jiangning District Analytical Instrument Factory; Cone calorimeter, FTT0030， FTT company in the UK.

1.3 Sample Preparation

According to the formula in Table 1, mix evenly on a double roll open mill at a blending temperature of 90℃, and then use a tablet press to pre-press for 5 minutes and hot press for 3 minutes at 110℃ to prepare 1 mm, 2 mm, and 3 mm sheet samples for experimental testing and analysis.

Table 1 Formula of composite materials

Sample	EVA/g	APP/g	Sepiolite/g	Mxene/g
EVA-0	50	0	0	0
EVA-A	40	10	0	0
EVA-AS	40	9.5	0.5	0
EVA-ASM	40	9.5	0.4	0.1

2 Results and Discussion

2.1 XRD

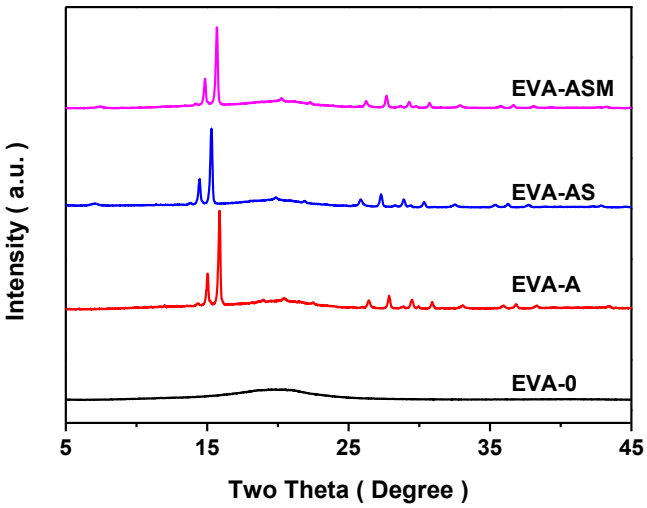
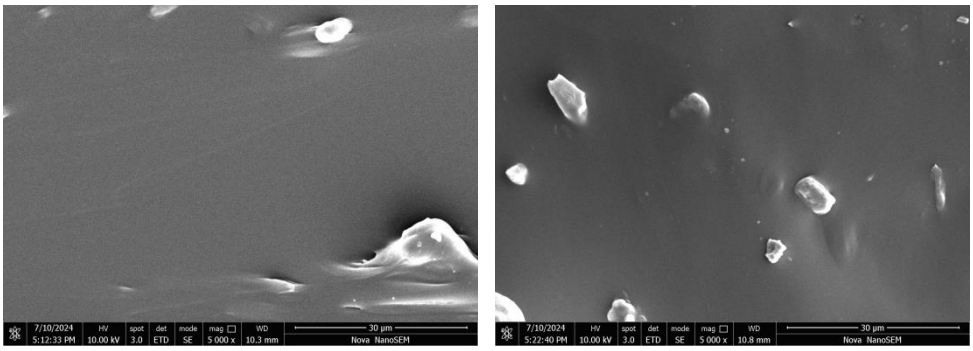


Fig.1. XRD curves of different EVA samples

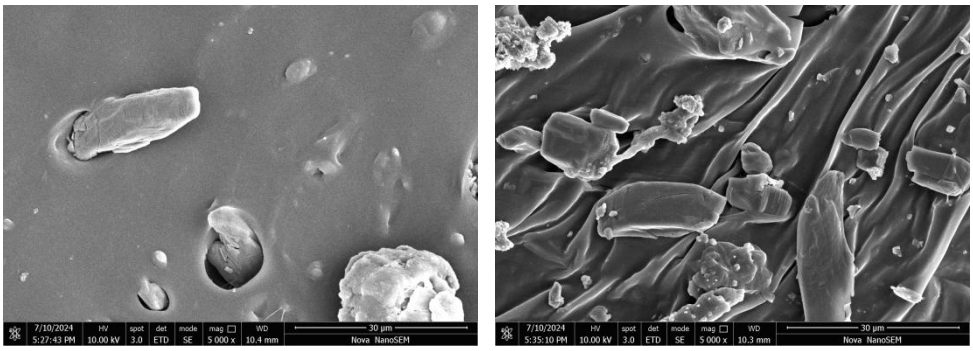
Fig.1 shows the XRD curves of different EVA samples. From the figure, it can be

seen that EVA exhibits a typical amorphous diffraction peak at 22.5°. The high content of vinyl acetate (VA) in EVA hinders the crystallization of the ethylene segment, resulting in lower crystallinity of EVA [26]. In the XRD curve of the EVA-A sample, strong diffraction peaks of 2θ appear at 15.3°, 27.5°, and 30.5°, corresponding to the crystal structure of ammonium polyphosphate (APP) [27]. At the same time, it can be seen that the peak position of EVA is shifted to the right, which may reflect the interaction between APP and EVA molecular chains (hydrogen bonding) [28]. Indicating that the APP interferes with the regular arrangement of EVA segments and reduces crystallinity. APP acts as a rigid particle that hinders EVA crystallization, but no new peak appears, indicating no chemical bonding. In the XRD curve of the EVA-AS sample, no characteristic peak of nano sepiolite at 7.4° (110 crystal plane) was observed [29]. Indicating that sepiolite has been peeled off or highly dispersed; At the same time, it can be observed that the EVA peak is further weakened, possibly due to the large specific surface area of sepiolite, which has an inhibitory effect on EVA crystallization. The leftward shift of the APP peak position may be due to the interaction between some sepiolite and APP through P-O-Si bonds. In the XRD curve of EVA-ASM samples, no characteristic peak of MXene (such as Ti_3C_2) at 6-9 ° (002 crystal plane) was observed [30]. Possible reasons may be that the content is too low, the X-ray signal is weak, or it may be due to shear force during the processing, resulting in partial peeling or increased interlayer spacing dispersed in EVA.

2.2 SEM



(a) (b)



(c) (d)

Fig.2. SEM images of different EVA samples

Fig.2 shows SEM images of cross-sections of different EVA samples. The cross-section of pure EVA is smooth and uniform, with typical ductile fracture characteristics (accompanied by wire drawing phenomenon). In Fig.2 (b), it can be seen that APP particles (1-5 μm) are dispersed in the matrix. Sepiolite is a nanofiber like structure with a diameter of 50-100nm. Due to the small amount of sepiolite added, it is evenly dispersed in the EVA substrate, without agglomeration, and tightly bonded to the substrate interface. In Fig.2 (d), more particles are observed, which are APP and MXene particles, and it can be seen that they are embedded by the polymer without stacking phenomenon.

2.3 Mechanical properties

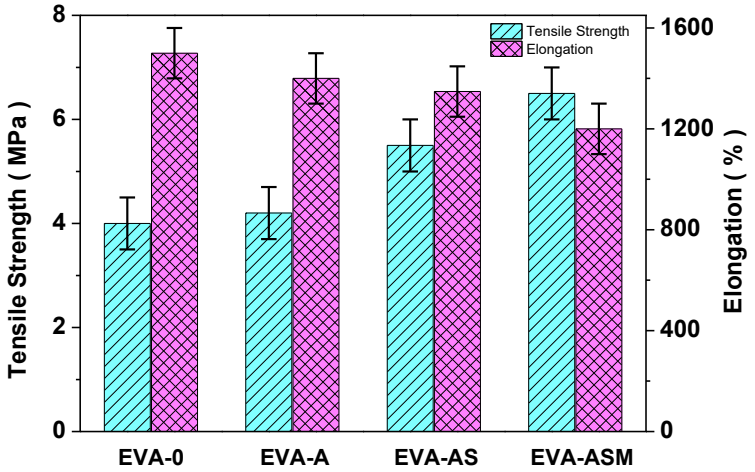


Fig.3. Variation of fracture elongation and fracture strength of different EVA samples

Fig.3 shows the tensile performance test results of different EVA samples. It can be seen from the figure that the elongation at break slowly decreases, from 1500% to

1200% And the tensile strength gradually increased, from 4 MPa to 6.8 MPa. The trend of mechanical property changes (decrease in elongation at break and increase in tensile strength at break) is very typical in polymer/filler composite systems, and the fundamental reason is that the addition of rigid fillers has a significant impact on the molecular chain movement and stress transfer mechanism of the EVA matrix. In the experiment, the sequential addition of APP， nano sepiolite and MXene reduces the ductility of the material by physically restricting the movement of EVA molecular chains, while significantly improving the rigidity or strength of the material through self bearing and effective stress transfer [31]. The sample EVA-ASM (containing MXene) has the highest tensile strength and the lowest elongation, reflecting the outstanding role of MXene two-dimensional layers in enhancing efficiency and limiting chain movement. The specific function is as follows: Pure EVA is a low crystalline elastomer with highly flexible molecular chains. It can undergo a wide range of slip, orientation, and crystal rearrangement during stretching, thus having a very high elongation at break (1500%) and low tensile strength. In sample EVA-A, ammonium polyphosphate is a rigid inorganic particle (micrometer scale). These hard particles are dispersed in the EVA matrix, becoming physical "obstacles" that hinder the free movement and sliding of EVA molecular chains. Molecular chains cannot fully stretch and rearrange during stretching as in pure matrices, resulting in a decrease in macroscopic plastic deformation ability and fracture elongation. Sample EVA-AS (containing nano sepiolite), nano sepiolite is a high aspect ratio nanofiber filler. Its huge specific surface area and rigid structure exert a stronger binding effect (interface effect) on the surrounding EVA molecular chains [32]. This constraint not only limits the movement of chain segments, but may also hinder the formation or destruction of crystal regions (consistent with the decrease in EVA diffraction intensity in XRD), further weakening the ductility of the matrix. Sample EVA-ASM (including MXene), MXene is an ultra-thin two-dimensional layer. Layers have a large specific surface area and strong physical barrier effect. They are embedded in the matrix like "nanowalls", greatly limiting the movement path of EVA molecular chains in three-dimensional space [33]. This limiting effect is stronger than particles and fibers, resulting in a further

decrease in elongation at break to 1200%. From the perspective of the increase in tensile strength, particle reinforcement (APP) is a mechanism in which hard particles bear stress and hinder crack propagation. Sepiolite with a high aspect ratio can more effectively transfer loads and act like a "steel bar". They can bridge cracks and prevent their rapid expansion. MXene layers have extremely high modulus and strength. They can not only bear huge stresses, but their two-dimensional planar structure can also significantly increase the interface area for load transmission, providing excellent reinforcement efficiency. Layering can also hinder the propagation of cracks perpendicular to the tensile direction [34]. Based on the XRD results, the addition of fillers resulted in a decrease in the crystallinity of EVA (weakened peak intensity). Although a decrease in crystallinity usually leads to a slight reduction in tensile strength, in this system, the strength enhancement effect brought by filler reinforcement far outweighs the negative impact of decreased crystallinity. In addition, nano fillers may act as heterogeneous nucleation sites, altering the crystalline morphology of EVA (such as generating smaller spherulites), and small-sized spherulites are beneficial for strength [35].

2.4 Volume resistivity

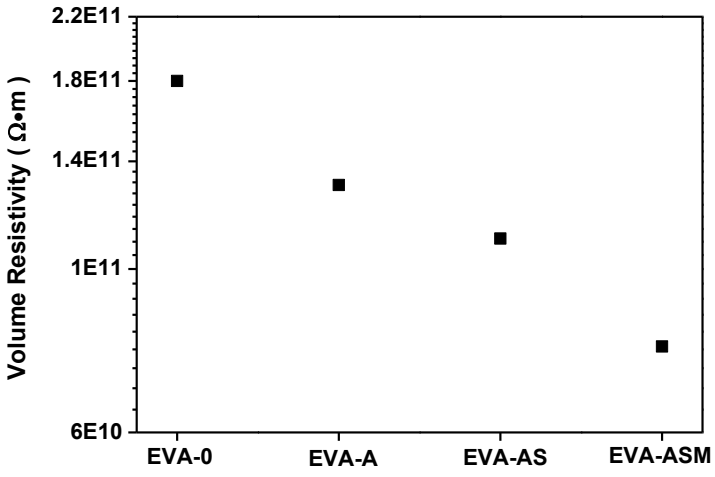


Fig.4. Volume resistivity of different EVA samples

Fig.4 shows the volume resistivity test results of different EVA samples. EVA itself is an excellent insulating polymer, and its volume resistivity is usually very high. The molecular chain structure lacks free electrons or ion carriers, making it difficult for

charges to migrate. Ammonium polyphosphate (APP) is an ionic flame retardant, but its solid crystal structure does not provide an electronic conductive path and has a high electrical resistivity (greater than $10^8\Omega\cdot m$). APP may undergo slight decomposition or moisture absorption during processing or testing, introducing a small amount of mobile ions (such as NH_4^+), resulting in extremely weak ion conductivity. The interface between APP particles and EVA matrix may become a location for charge accumulation and polarization, which may exhibit increased dielectric loss under AC testing, resulting in a slight decrease in resistivity compared to pure EVA. Nano sepiolite is a magnesium silicate mineral and also an insulator (with a resistivity greater than $10^{12}\ \Omega\cdot cm$). The mechanism that leads to the decrease in resistivity may be: 1) reducing crystallinity and increasing amorphous region, as shown by XRD, the addition of sepiolite further inhibits EVA crystallization. The amorphous region has higher molecular chain activity, which may be more conducive to the migration of trace ions introduced by the aforementioned APP. 2) Forming more complex interfaces, the huge specific surface area and nanofiber morphology of sepiolite form more interfaces with APP particles and EVA matrix [36]. These interface regions may adsorb trace amounts of moisture or impurity ions. Becoming a charge trap or promoting interface polarization (especially in alternating current fields). 3) Potential ion channels, the crystal structure of sepiolite contains exchangeable cations (such as the position where Mg^{2+} is replaced by Na^+/Ca^{2+}), which theoretically may have weak ion conductivity under specific conditions (such as high humidity), but contribute very little in dry polymer composites. MXene materials have metallic like conductivity, with an intrinsic conductivity of 10000-20000 S/cm (resistivity as low as about $5\times10^{-5}\Omega\cdot cm$), which is about 20 orders of magnitude higher than polymer matrices [37]. In theory, it can significantly reduce the resistivity of EVA. Although APP and nano sepiolite are insulators themselves, their presence plays a key role in the dispersion of MXene and the construction of the final conductive network, leading to a trend of "slow decline" rather than "sudden drop".

2.5 TGA

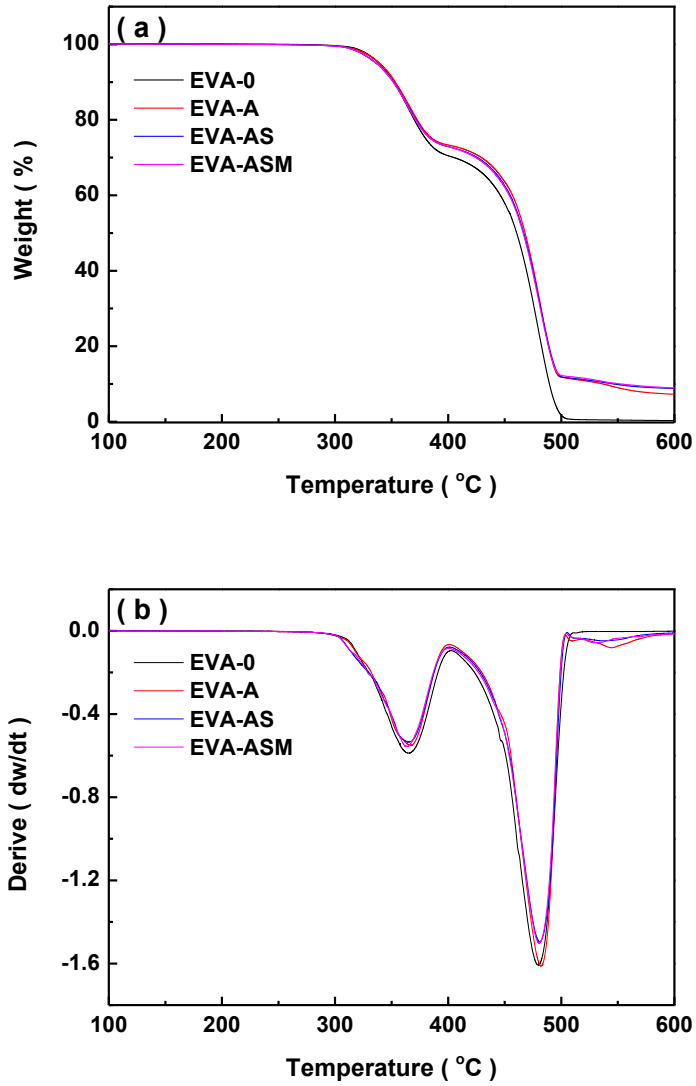


Fig.5. Thermogravimetric curves of different EVA samples (a, TGA; b, DTG)

Table 2 data from TGA

Samples	$T_{10\%}$/°C	T_{max1}/°C	T_{max2}/°C	Yield/%
EVA-0	351.9	365.5	479.6	0.3
EVA-A	353.2	367.1	482.3	7.3
EVA-AS	351.7	365.9	481.1	8.8
EVA-ASM	351.4	363.9	480.6	9.0

Fig.5 shows the thermogravimetric curves of different EVA samples. There are two decomposition stages in the TGA curve of EVA samples, which are the thermal decomposition of the side chains (around 365℃) and the main chain (around 480℃) of EVA [38]. The temperature at which 10% weight loss occurs is defined as the initial

decomposition temperature, and the maximum thermal decomposition temperatures of the side chains and main chains of EVA are T_{max1} and T_{max2}, respectively. The phenomenon in TGA where the initial decomposition temperature and maximum decomposition temperature first increase and then decrease. APP acts as an acid source and decomposes into polyphosphoric acid (PPA) at lower temperatures (approximately 250-300℃). PPA acts as a strong Lewis acid catalyst for the deacetylation of EVA, accelerating the removal of acetic acid (below the decomposition temperature of pure EVA). At the same time, it promotes dehydration cross-linking into carbon, allowing EVA molecular chains to crosslink at lower temperatures and form a more thermally stable carbon layer [39,40]. Overall, the addition of the app has changed the thermal decomposition pathway of EVA. Although the initial decomposition (deacidification) may occur slightly earlier, the occurrence of carbonization reaction significantly increases the amount of heat required for main chain breakage (severe weight loss stage). The physical barrier formed by the carbon layer on the surface also delays the further decomposition of the internal matrix, resulting in a shift of the severe weight loss peak (T_{max2}) towards higher temperatures. The huge specific surface area and surface silicon hydroxyl groups (-Si-OH) of nano sepiolite may adsorb a portion of the polyphosphate (PPA) or reaction intermediates produced by APP decomposition, which "binds" the catalytic activity of PPA in the short term. Sepiolite, as an inert filler, occupies a certain volume and may slightly reduce the concentration of active catalytic components (PPA) per unit volume. The physical adsorption and dilution of PPA by sepiolite may slightly inhibit the catalytic efficiency of APP in the early stage of decomposition, leading to a slightly earlier severe decomposition stage (compared to sample EVA-A). But this effect is weak, so the decrease is very small (only 1.2℃). The addition of MXene will shift the intense char decomposition reaction (severe weight loss stage) towards lower temperatures as a whole. Although decomposition begins earlier, the carbon layer generated by catalysis forms earlier and of higher quality. This carbon layer can more effectively protect the remaining matrix, which may lead to a slower weight loss rate and an increase in residual carbon rate during the later decomposition stage (high temperature zone). Therefore, the decrease in T_{max}

(maximum weight loss rate temperature) does not represent a deterioration in thermal stability, but rather the result of efficient catalytic reshaping of the decomposition pathway. In TGA testing, the carbon residue rate increased sequentially, reaching 0.3%, 7.3%, 8.8%, and 9.0%, respectively. The stepwise growth of residual carbon rate is an inevitable result of the upgrading and collaborative optimization of flame retardant systems layer by layer. The APP provides the basic catalytic ability to produce carbon, achieving from scratch (0.3% to 7.3%). Nano sepiolite enhances the stability of the carbon layer through physical enhancement and chemical synergy (P-O-Si) by 7.3% to 8.8%. MXene, with its superior catalytic activity (Ti^{4+}) and two-dimensional structure advantages [41], further optimizes the carbonization efficiency and char layer quality (8.8% to 9.0%) when approaching the upper limit. Although its contribution is the smallest in numerical terms, it is a key leap towards achieving top-level flame retardant performance (highest LOI value).

2.6 LOI

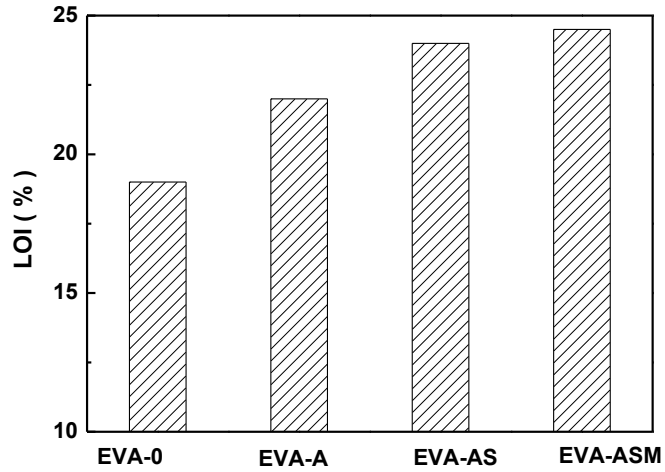


Fig.6. LOI values of different EVA samples

Fig.6 shows the variation of LOI values for different EVA samples. As shown in the figure, with the gradual addition of flame retardants, the LOI of EVA samples gradually increases. APP is a classic expansion type flame retardant that acts as a physical barrier during combustion. The expanded carbon layer isolates oxygen from diffusing into the substrate and blocks heat transfer to the interior. The non combustible gases produced by combustion dilute the fuel and oxygen concentrations in the gas-

phase combustion zone [42]. In addition, the APP can also suppress droplets, increase the viscosity of the melt through the carbon layer, and reduce the ignition of droplets from other substances. Sepiolite is a carbon layer enhancer and synergist, physically enhancing the "skeleton": the nanofiber structure of sepiolite is embedded in the expanded carbon layer, like "steel bars", to enhance the strength of the carbon layer and prevent it from collapsing and breaking under the impact of heat or air flow. The silicon hydroxyl groups (-Si-OH) on the surface of sepiolite may react with polyphosphate produced by APP decomposition to form P-O-Si bonds. This not only stabilizes polyphosphate and prolongs its catalytic activity, but may also promote the formation of more stable and higher graphitized carbon layers [43,44]. MXene is an emerging two-dimensional flame retardant and catalytic material with excellent physical barrier properties, which effectively blocks oxygen permeation and heat feedback. Efficient heat conduction and dissipation during the combustion process. MXene has ultra-high planar thermal conductivity, which can quickly diffuse the heat in the combustion zone laterally, reduce the local temperature on the material surface, and suppress pyrolysis and combustion. Catalytic carbonization and carbon layer modification to increase residual carbon content. Promoting graphitization, the carbon layer formed by catalysis has a higher degree of graphitization, is more stable, and more resistant [44]. In synergy with APP and sepiolite, MXene may promote the formation of P-O-Ti bonds between APP and sepiolite systems, constructing an "organic-inorganic hybrid" carbon layer with significantly improved strength, density, and thermal stability (ternary synergistic effect). In addition, MXene components may capture free radicals (·H, ·OH) in combustion chain reactions, inhibiting gas-phase combustion. In summary, the gradual increase in LOI is the inevitable result of the complementary and deep synergy of APP (expanded to carbon basis), nano sepiolite (carbon layer enhancement and synergistic catalysis), and MXene (top-level two-dimensional barrier, efficient catalytic carbonization, thermal conductivity and heat dissipation).

2.7 Cone calorimeter

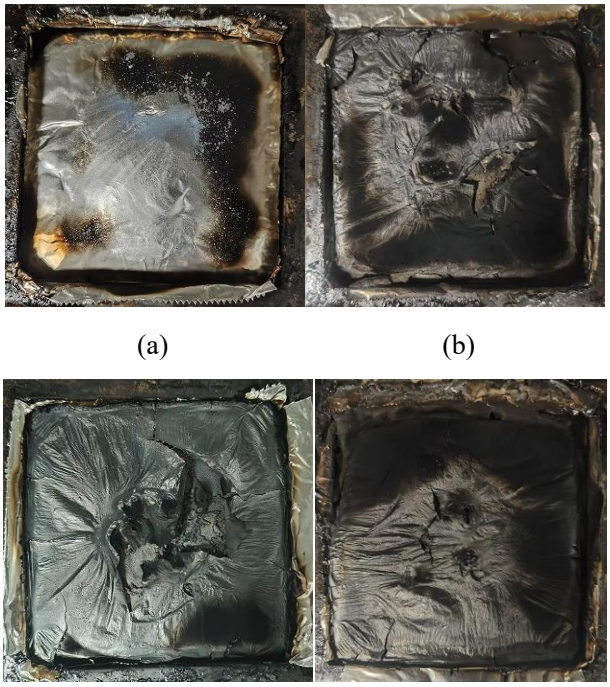


Fig.7. Optical images of ash after combustion of different EVA samples

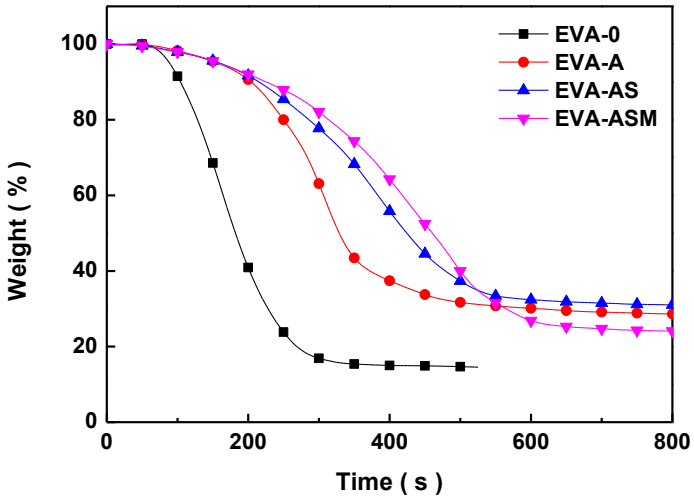


Fig.8. Combustion quality loss curves of different EVA samples

The combustion behavior of different EVA samples was tested using a cone calorimeter. Fig.7 shows the ash images of different EVA samples after combustion. It can be seen that pure EVA is completely burned with almost no residue, and the combustion mass loss curve also rapidly decreases (Fig.8), showing a high combustion rate. Sample EVA-A (including APP), light gray, porous residual carbon, APP decomposes to produce polyphosphate (PPA), catalyzing EVA dehydration crosslinking to form an expanded carbon layer. Sample EVA-AS (including APP and sepiolite)

leaves a structurally intact gray black block like residual carbon after combustion, which is not easily fragmented. Sepiolite fibers are embedded as a "skeleton" in the carbon layer, reducing the merging of pores and structural collapse [45]. After the combustion of sample EVA-ASM, a deep black, smooth, dense and relatively intact residual carbon is left behind, and there is a metallic sound when struck. MXene layers migrate to the surface to form a "ceramicized" dense barrier, and ternary synergy (P-O-Ti bonds, etc.) is used to construct organic-inorganic hybrid carbons with extremely high thermal stability [46]. Due to the catalytic effect, the degree of graphitization is high, resulting in a deep black color. Due to the above reasons, the rate of combustion quality loss of the sample gradually decreases (as shown in Fig.8).

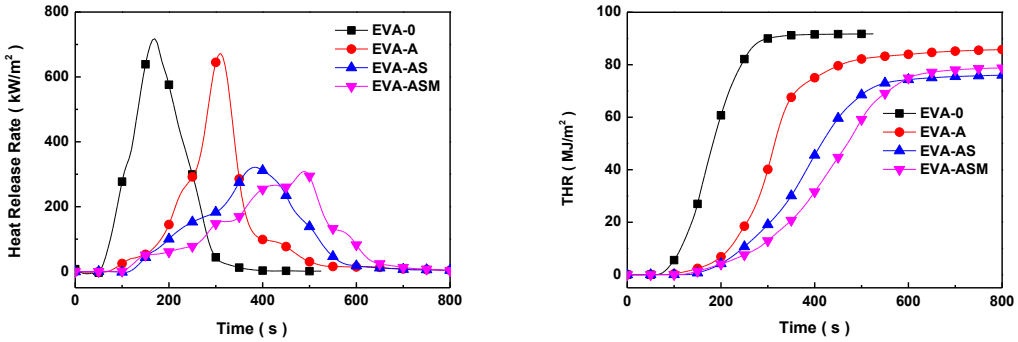


Fig.9. HRR and THR curves of different EVA samples during combustion

Fig.9 shows the heat release rate (HRR) and the total heat release (THR) curves of different EVA samples during combustion. It can be seen that in the cone calorimeter test, the maximum heat release peak in the heat release rate curve (HRR) shifts backwards in sequence, and the peak heat release rate (pHRR) decreases from 718 kW/m^2 to 308 kW/m^2. The total heat release (THR) decreases sequentially, from 91.7 MJ/m^2 of EVA to 74.7 MJ/m^2. The shift of the HRR peak in Fig.9 (a) reflects the gradual delay of the combustion process. This is because starting from sample EVA-A, the flame retardant (APP) and its synergistic components (sepiolite, Mxene) formed an increasingly effective, stable, and durable physical barrier layer (expanded carbon layer) on the material surface. This barrier layer greatly delays the transfer of heat to the internal matrix and the transport of internal combustible volatiles to the flame zone, resulting in a longer time required to reach the maximum heat release rate after ignition

[47-50]. The more flame retardants added, the better the synergistic effect, the higher the barrier layer efficiency formed, and the more obvious the delay effect. In Fig.9(b), THR decreases sequentially, reflecting the increasingly incomplete combustion process. The presence of efficient barrier layers (especially samples EVA-AS and EVA-ASM) greatly limits the release of flammable volatiles and the supply of oxygen to the interior of the material. A large amount of carbonaceous material is retained in the condensed phase to form a char layer, rather than being converted into combustible gas and burned off. Meanwhile, the catalytic effect of Mxene significantly improves the carbonization efficiency, further reducing the generation of combustible gases. Therefore, the total amount of substances that can completely burn and release heat decreases sequentially, leading to a stepwise decrease in THR [51].

Conclusion

This study successfully constructed an APP/NS/MXene/EVA ternary synergistic flame retardant system by introducing nano sepiolite (NS) and MXene step by step. The main conclusions are as follows:

(1) The XRD results showed that no new peaks appeared in different EVA samples, indicating no chemical bonding. The SEM results indicate that the flame retardant particles are evenly dispersed in the EVA substrate, without agglomeration, and tightly bonded to the matrix interface.

(2) The results of mechanical performance testing and volume resistivity testing show that the introduction of NS/MXene increases the fracture strength from 4 MPa to 6.8 MPa. The volume resistivity slowly decreases, but remains greater than 10^{10} Ω·cm.

(3) The LOI test results showed that MXene, due to its catalytic graphitization of the carbon layer, synergistically increased the LOI from 18% to 24.5% with NS.

(4) TGA indicates that the catalytic effect of MXene reduces the maximum weight loss temperature, but increases the residual carbon rate to 9.0%.

(5) The CONE test showed that the maximum heat release peak in the heat release rate (HRR) shifted backwards in sequence, while the total heat release (THR) decreased in sequence.

CRediT authorship contribution statement

Xuezheng Huang:Funding acquisition,Project administration,Writing-review & editing. Zhipeng Hou: Investigation, Methodology, Writing-original draft. Feng Liang:Investigation, Methodology. Junfeng Tian:Investigation, Methodology. Jianxi Li: Investigation, Data curation, Formal analysis. Li Wu: Funding acquisition, Project administration, Writing-review &editing

Data availability

Data availability Data will be made available on request.

Declaration of Competing Interest

The authors declare that they have no known competing financial interests or personal relationships that could have appeared to influence the work reported in this paper.

Acknowledgements

Financial support of the Natural Science Foundation of Henan (Grant No.242300420012),the Natural Science Foundation of Henan (Grant No.262300421317) .

References

1. Wang GH, He ML, Chai FC, Feng JD, Dai YD (2019) Enhancement of flame retardancy and radiation shielding properties of ethylene vinyl acetate based radiation shielding composites by EB irradiation, Prog. Nucl. Energy 112:225-232. https://doi.org/10.1016/j.pnucene.2019.01.001.
2. Xu SY, Li JX, Ye QF, Shen LG, Lin HJ (2021) Flame-retardant ethylene vinyl acetate composite materials by combining additions of aluminum hydroxide and melamine cyanurate: Preparation and characteristic evaluations, J. Colloid Interface Sci. 589:525-531. https://doi.org/10.1016/j.jcis.2021.01.026.
3. Czanderna AW, Pern FJ (1996) Encapsulation of PV modules using ethylene vinyl acetate copolymer as a pottant: A critical review, Sol. Energy Mater. Sol. Cells 43(2):101-181. https://doi.org/10.1016/0927-0248(95)00150-6.
4. Feng CM, Liang MY, Jiang JL, Liu HB, Huang JG (2016) Huang, Synergistic effect of ammonium polyphosphate and triazine-based charring agent on the flame retardancy and combustion behavior of ethylene-vinyl acetate copolymer, J. Anal. Appl. Pyrolysis 119:259-269. https://doi.org/10.1016/j.jaap.2016.01.004.

5. Xu SY, Han Y, Zhou C, Li JX, Shen LG, Lin HJ (2023) Lin, A biobased flame retardant towards improvement of flame retardancy and mechanical property of ethylene vinyl acetate, Chin. Chem. Lett. 34(1):107585. https://doi.org/10.1016/j.cclet.2022.02.008.
6. Trivedi HK, Meshram A, Gupta R (2024) Removal of encapsulant Ethylene-vinyl acetate (EVA) from solar cells of photovoltaic modules (PVMs), Mater. Today Proc. 112:73-76. https://doi.org/10.1016/j.matpr.2023.08.109.
7. Chen SG, Yu HY, Wang RY, Zhang Y (2008) Research progress of halogen-free flame-retardants in ethylene-vinyl acetate copolymer, China Plastics 22(4):13-20. https://doi.org/10.19491/j.issn.1001-9278.2008.04.003.
8. Tang WF, Zhang HM, Liu T, Li XL, Yang H, Huang WZ, Liao YH, Gu XY, Zhang S (2024) Improving the flame retardancy and smoke suppression of ethylene vinyl acetate composites by introducing the hybrid material of Zn/TiO_2@AKaol, Polym. Degrad. Stab. 221:110673. https://doi.org/10.1016/j.polymdegradstab.2024.110673.
9. Jiang XC, Li P, Liu Y, Wang JS (2023) Wang, Flame-retardant ramie fabrics with APP: flame retardancy, flame-retardant mechanism and mechanical properties, Cellulose 30(2):1321-1334. https://doi.org/10.1007/s10570-022-04962-3.
10. Qin RH, Song YH, Niu M, Xue BX, Liu LY (2020) Construction of flame retardant coating on polyester fabric with ammonium polyphosphate and carbon microspheres, Polym. Degrad. Stab. 171:109028. https://doi.org/10.1016/j.polymdegradstab.2019.109028.
11. Jeencham R, Suppakarn N, Jarukumjorn K (2014) Effect of flame retardants on flame retardant, mechanical, and thermal properties of sisal fiber/polypropylene composites, Composites, Part B 56:249-253. https://doi.org/10.1016/j.compositesb.2013.08.012.
12. Liu T, Jing J, Zhang Y, Fang ZP (2018) Synthesis of a novel polyphosphate and its application with APP in flame retardant PLA, RSC Adv. 8(8):4483-4493. https://doi.org/10.1039/c7ra12582h.
13. Liu Y, Wang JS, Deng CL, Wang DY, Song YP, Wang YZ (2010) The synergistic flame-retardant effect of O-MMT on the intumescent flame-retardant PP/CA/APP systems, Polym. Adv. Technol. 21(11):789-796. https://doi.org/10.1002/pat.1502.
14. Wang ZY, Han EH, Ke W (2005) Influence of nano-LDHs on char formation and fire-resistant properties of flame-retardant coating, Prog. Org. Coat. 53(1):29-37.

https://doi.org/10.1016/j.porgcoat.2005.01.004.

15. Wang X, Guo WW, Cai W, Wang JL, Song L, Hu Y (2020) Recent advances in construction of hybrid nano-structures for flame retardant polymers application, Appl. Mater. Today 20:100762. https://doi.org/10.1016/j.apmt.2020.100762.
16. Chikh A, Benhamida A, Kaci M, Pillin I, Bruzaud S (2016) Synergistic effect of compatibilizer and sepiolite on the morphology of poly (3-hydroxybutyrate-co-3-hydroxyvalerate)/poly (butylene succinate) blends, Polym. Test. 53:19-28. https://doi.org/10.1016/j.polymertesting.2016.05.008.
17. Beauger C, Lainé G, Burr A, Taguet A, Otazaghine B (2015) Improvement of Nafion®-sepiolite composite membranes for PEMFC with sulfo-fluorinated sepiolite, J. Membr. Sci. 495:392-403. https://doi.org/10.1016/j.memsci.2015.08.014.
18. Tan SM, Li YT, Xu LJ, Xin ZX, Zhao S, Wang H, Li L (2024) Development of SEP based coeffective flame retardant and its smoke suppression for EPDM, J. Polym. Res. 31(9):252. https://doi.org/10.1007/s10965-024-04099-w.
19. Núñez K, Gallego R, Pastor JM, Merino JC (2014) The structure of sepiolite as support of metallocene co-catalyst during in situ polymerization of polyolefin (nano)composites, Appl. Clay Sci. 101:73-81. https://doi.org/10.1016/j.clay.2014.07.020.
20. Henriques RR, Soares BG (2020). SEP modified with phosphonium ionic liquids as anticorrosive pigment for epoxy coatings, Appl. Clay Sci. 200:105890-105898. https://doi.org/10.1016/j.clay.2020.105890.
21. Liu Y, Zhao J, Deng CL, Chen L, Wang DY, Wang YZ (2011). Flame-retardant effect of sepiolite on an intumescent flame-retardant polypropylene system, Ind. Eng. Chem. Res. 50(4):2047-2054. https://doi.org/10.1021/ie101737n.
22. Lim KRG, Shekhirev M, Wyatt BC, Anasori B, Gogotsi Y, Seh ZW (2022). Fundamentals of MXene synthesis, Nat. Synth. 1(8):601-614. https://doi.org/10.1038/S44160-022-00104-6.
23. Zhou JY, Tang SY, Wang L, Peng LL, Liu QL, Kang JB, Gohi BFCA, Xu S (2026) Constructing 2D/1D sepiolite/$Ti_3C_2T_x$ heterostructures for multifunctional EVA composites: cooperative enhancement in fire safety, thermal conductivity, and antibacterial activity, Polym. Degrad. Stab. 248:112058. https://doi.org/ 10.1016/j.polymdegradstab.2026.112058.
24. Ma L, Wang YD, Gao JJ, Zhu ZM (2024) Construction of MXene-based flame retardant with

multiple carbonization towards for reducing fire hazard and smoke release of epoxy resin, Eur. Polym. J. 215:113253. https://doi.org/10.1016/j.eurpolymj.2024.113253.

25. Chen WH, Liu PJ, Liu Y, Liu ZX (2022) Recent advances in two-dimensional $Ti_3C_2T_x$ MXene for flame retardant polymer materials, Chem. Eng. J. 446:137239. https://doi.org/10.1016/j.cej.2022.137239.
26. Ferreira EDB, Luna CBB, Siqueira DD, Araújo EM, de França DC, Wellen RMR (2022) Annealing effect on PLA/EVA blends performance, J. Polym. Environ. 30(2):1-14. https://doi.org/10.1007/s10924-021-02220-4.
27. Prabhakar MN, Raghavendra GM, Vijaykumar BVD, Patil K, Seo J, Jung-il S (2019) Synthesis of a novel compound based on chitosan and ammonium polyphosphate for flame retardancy applications, Cellulose 26(16):8801-8812. https://doi.org/ 10.1007/s10570-019-02671-y.
28. Wang BB, Tang QB, Hong NN, Song L, Wang L, Shi YQ, Hu Y (2011) Effect of cellulose acetate butyrate microencapsulated ammonium polyphosphate on the flame retardancy, mechanical, electrical, and thermal properties of intumescent flame-retardant ethylene–vinyl acetate copolymer/microencapsulated ammonium polyphosphate/polyamide-6 blends, ACS Appl. Mater. Interfaces 3(9):3754-3761. https://doi.org/10.1021/am200940z.
29. Darvishi Z, Morsali A (2010) Synthesis and characterization of nano-sepiolite by solvothermal method, Appl. Surf. Sci. 256(11):3607-3611. https://doi.org/10.1016/j.apsusc.2009.12.163.
30. Huang JHR, Tseng SW, Chen IWP (2025) In-situ electrochemical XRD and Raman probing of ion transport dynamics in ionic liquid-etched $Ti_3C_2T_x$ MXene for energy storage applications, Chem. Eng. J. 503:158232. https://doi.org/10.1016/j.cej.2024.158232.
31. Jotiram GA, Palai BK, Bhattacharya S, Aravinth S, Gnanakumar G, Subbiah R, Chandrakasu M (2022) Investigating mechanical strength of a natural fibre polymer composite using SiO_2 nano-filler, Mater. Today Proc. 56:1522-1526. https://doi.org/10.1016/j.matpr.2022.01.176.
32. Feng Y, Wang Q, Yang XC (2024) Study on micro-mechanical properties of EVA modified rubber-cementitious materials based on molecular dynamics simulation, Constr. Build. Mater. 416:135132. https://doi.org/10.1016/j.conbuildmat.2024.135132.
33. Yan L, Xu ZS, Wang XH (2017) Influence of nano-silica on the flame retardancy and smoke suppression properties of transparent intumescent fire-retardant coatings, Prog. Org. Coat. 112:319-329. https://doi.org/10.1016/j.porgcoat.2017.07.017.

34. Shi YQ, Liu C, Duan ZP, Yu B, Liu MH, Song PA (2020) Interface engineering of MXene towards super-tough and strong polymer nanocomposites with high ductility and excellent fire safety, Chem. Eng. J. 399:125829. https://doi.org/10.1016/j.cej.2020.125829.
35. Galeski A (2003) Strength and toughness of crystalline polymer systems, Prog. Polym. Sci. 28(12):1643-1699. https://doi.org/10.1016/j.progpolymsci.2003.09.003.
36. Seo MK, Park SJ (2004) Electrical resistivity and rheological behaviors of carbon nanotubes-filled polypropylene composites, Chem. Phys. Lett. 395(1-3):44-48. https://doi.org/10.1016/j.cplett.2004.07.047.
37. Kadam SA, Kadam KP, Pradhan NR (2024) Advancements in 2D MXene-based supercapacitor electrodes: synthesis, mechanisms, electronic structure engineering, flexible wearable energy storage for real-world applications, and future prospects, J. Mater. Chem. A 12(29):17992-18046. https://doi.org/10.1039/d4ta00328d.
38. Wang YS, Ye W, Jiang Y, Wang DY (2025). Triethylenetetramine-modified ammonium polyphosphate as charring agent for enhanced flame retardancy in ethylene vinyl acetate copolymer, Advanced Industrial and Engineering Polymer Research 8:433-442. https://doi.org/10.1016/j.aiepr.2025.05.004.
39. Dai JF, Li B (2010) Synthesis, thermal degradation, and flame retardance of novel triazine ring-containing macromolecules for intumescent flame retardant polypropylene, J. Appl. Polym. Sci. 116(4):2157-2165. https://doi.org/10.1002/app.31813.
40. Xie HL, Lai XJ, Li HQ, Zeng XR (2016) Synthesis of a novel macromolecular charring agent with free-radical quenching capability and its synergism in flame retardant polypropylene, Polym. Degrad. Stab. 130:68-77. https://doi.org/10.1016/j.polymdegradstab.2016.05.029.
41. Zhong Q, Li Y, Zhang G (2021) Two-dimensional MXene-based and MXene-derived photocatalysts: recent developments and perspectives, Chem. Eng. J. 409:128099. https://doi.org/10.1016/j.cej.2020.128099.
42. Xu YJ, Qu LY, Liu Y, Zhu P (2021) An overview of alginates as flame-retardant materials: pyrolysis behaviors, flame retardancy, and applications, Carbohydr. Polym. 260:117827. https://doi.org/10.1016/j.carbpol.2021.117827.
43. Shao ZB, Deng C, Tan Y, Chen MJ, Chen L, Wang YZ (2014) An efficient mono-component polymeric intumescent flame retardant for polypropylene: preparation and application, ACS

Appl. Mater. Interfaces 6(10):7363-7370. https://doi.org/10.1021/am500789q.

44. Idumah CI (2023) Recently emerging advancements in thermal conductivity and flame retardancy of MXene polymeric nanoarchitectures, Polym.-Plast. Technol. Mater. 62(4):510-546. https://doi.org/10.1080/25740881.2022.2121220.
45. Zhao D, Xia ML, Shen YC, Wang TW (2019) Three-dimensional cross-linking structures in ceramifiable EVA composites for improving self-supporting property and ceramifiable properties at high temperature, Polym. Degrad. Stab. 162:94-101. https://doi.org/10.1016/j.polymdegradstab.2019.02.003.
46. Luo Y, Xie YH, Geng W, Dai GF, Sheng XX, Xie DL, Wu H, Mei Y (2022) Fabrication of thermoplastic polyurethane with functionalized MXene towards high mechanical strength, flame-retardant, and smoke suppression properties, J. Colloid Interface Sci. 606(Pt 1):223-235. https://doi.org/10.1016/j.jcis.2021.08.025.
47. Idumah CI, Ezeani EO, Ezika AC, Timothy UJ (2021) Recent advancements in flame retardancy of MXene polymer nanoarchitectures, Saf. Extreme Environ. 3(3):1-21. https://doi.org/10.1007/S42797-021-00046-W.
48. Feng YL, Wu W, Wang ZY, Zhao TY (2022) POSS-modified ammonium polyphosphate for improving flame retardant of epoxy resins, Polym. Adv. Technol. 33(4):1190-1201. https://doi.org/10.1002/pat.5592.
49. Xu J, Niu YJ, Xie ZP, Liang F, Guo FH, Wu JJ (2023) Synergistic flame retardant effect of carbon nanohorns and ammonium polyphosphate as a novel flame retardant system for cotton fabrics, Chem. Eng. J. 451:138566. https://doi.org/10.1016/j.cej.2022.138566.
50. Deng CL, Deng C, Zhao J, Li RM, Fang WH, Wang YZ (2015) Simultaneous improvement in the flame retardancy and water resistance of PP/APP through coating UV-curable pentaerythritol triacrylate onto APP, Chin. J. Polym. Sci. 33(2):203-214. https://doi.org/10.1007/s10118-015-1575-5.
51. Gao JJ, Wang YD, Ma L, Zhu ZM, Xiao F (2025) Phosphorus-functionalized MXene nanohybrid toward fire-resistant, mechanically reinforced and toughened PLA composites, Polym. Degrad. Stab. 239:111392. https://doi.org/10.1016/j.polymdegradstab.2025.111392.

Supplementary Files

This is a list of supplementary files associated with this preprint. Click to download.

- Supplementarymaterial.docx